International Journal of Thin Films Science and Technology

http://dx.doi.org/10.18576/ijtfst/050109

Performance of Transparent Conducting Fluorine-doped Tin Oxide Films for Applications in Energy Efficient Devices

A. E. Hassanien[1], *H. M. Hashem*[1,*], *G. Kamel*[1], *S. Soltan*[1], *A. M. Moustafa*[2], *M. Hammam*[1] *and A. A. Ramadan*[1].

[1] Physics Department, Faculty of Science, Helwan University, Helwan, Egypt.
[2] Solid State Physics Department, National Research Center, Dokki, Cairo, Egypt.

Received: 15 Nov. 2015, Revised: 7 Dec. 2015, Accepted: 15 Dec. 2015.
Published online: 1 Jan. 2016.

Abstract: Un-doped and fluorine-doped tin oxide (F:SnO_2) films were prepared by spray pyrolysis technique on glass substrates. A systematic optimization of the solvent and the precursor as well as the preparation parameters and their effect on structural and physical (electrical/optical) characteristics are investigated. Although a single phase of tetragonal structure is obtained under all the preparation parameters, the type of crystallographic preferred orientation is mainly dependent on the solvent and the doping level. The crystallite size is in the range of 15-25 nm. The increase of spray time, substrate temperature and solution concentration results in an increase in the film thickness and a decrease in the sheet resistance. The average transmission has been found to change from 60 % to 90 % depending upon the variation of spray time and solution concentration. According to values of the figure of merit ($\Phi_{TC} = T_{550}^{10} / R_s$), the optimum preparation parameters are: propanol as a solvent, spray time of 2 min, substrate temperature of 500 °C and solution concentration of 0.3 M. Considering these optimum preparation conditions fluorine-doped SnO_2 was prepared and the highest figure of merit of value ≈ 8.5×10^{-3} Ω^{-1} is specified at 27 at. %.

Keywords: spray pyrolysis, transparent electrodes, fluorine-doped tin oxide (FTO), materials for energy, structure characteristics (XRD), electric/optical investigations

1 Introduction

Transparent conductive oxide films are common components of energy devices in photovoltaic technology and electrochromic functional materials as well as in varieties of useful applications in the area of smart energy materials. One of the main layers that affect the performance of these devices are the transparent electrode thin films. Transparent conducting oxides, TCO, are wide band gap semiconductors (≥ 3.1 eV) and whose properties strongly depend on the deposition technique and the preparation conditions. [1-2] TCO's form a group of materials having a very interesting combination of high visible transparency and high electrical conductivity. [3-5] This in turn makes them widely applicable in a variety of optoelectronic devices such as solar cells as well as display and electrochromic devices. [6-8] Among the transparent conducting films, fluorine-doped tin oxide (F:SnO_2) ones are the most interesting due to their high chemical stability, mechanical strength and thermal resistance as well as their low cost. These properties nominate F:SnO_2 as one of the most promising candidate for gas sensors [9], photovoltaic solar energy conversion [10-11], heat mirrors [12] and electrochromic devices [13]. Many deposition techniques were involved, such as spray pyrolysis [14-17], sol-gel coatings [18], plasma-enhanced chemical vapor deposition (PECVD) [19] and R.F. magnetron-sputtering [20].

The choice of a particular materials is, generally, based on a set of performance requirements such as electrical, magnetic, optical and mechanical properties in addition to its physical, chemical and thermal stability. Two parameters, the optical transmission (T) and sheet resistance (Rs), characterize the transparent conducting oxides and have to be optimized for the thin film coatings. Depending on the type of the required device, the optical transmission and the electrical conduction of the transparent electrode will have to exceed certain minimum value and, if possible, both parameters should be as high as possible. However, higher conductivity usually causes lower transmission due to the thicker film layer. In order to compare the performance of transparent conductor materials, a meaningful figure of merit has to be defined. Up till now, the figure of merit, ϕ_{TC}, defined by Haacke, is considered since it provides the most favorable choice as a practical useful tool for comparing the performance of transparent conductive coatings. [21] This is calculated by Haacke formula given as:

$$\phi_{TC} = T_{550}^{10} / R_s$$

*Corresponding author E-mail: hany_m_hashem@yahoo.com

where T_{550} is the transmission at $\lambda = 550$ nm. It is well known that thin film characteristics may vary from one laboratory to another and that they are very sensitive to the preparation parameters even within the same laboratory. However, optimization of preparation parameters and discussion of their effect on the characteristics of the prepared films are required and useful in any case. This work aims at the study of the performance of transparent conductive electrodes by a systematic optimization of the liquid precursor solution and the preparation parameters of un-doped and fluorine-doped tin oxide using the spray pyrolysis method as economic, simple and fast deposition technique that serving for many applications. The effect of the deposition conditions on the structural (phase identification, crystallite size and crystallographic texture) and the physical (electrical/optical) characteristics will be investigated and correlated for the preparation of high performance transparent electrodes that can be used in energy efficient devices.

2. Experimental

2.1. Materials

2.1.1. SnO_2 films

Two inorganic tin compounds stannic chloride ($SnCl_4.5H_2O$) and anhydrous stannous chloride ($SnCl_2$) were chosen as the precursor to prepare the undoped tin oxide (SnO_2) thin films. In addition, two different solvents are used; water and isopropyl alcohol (2-propanol).

2.1.2. Fluorine-doped tin oxide (FTO) films

Ammonium fluoride (NH_4F) was used considering the optimum preparation parameters of SnO_2; precursor, solvent, spray time, substrate temperature and solution concentration.

2.2. Thin Film Preparation

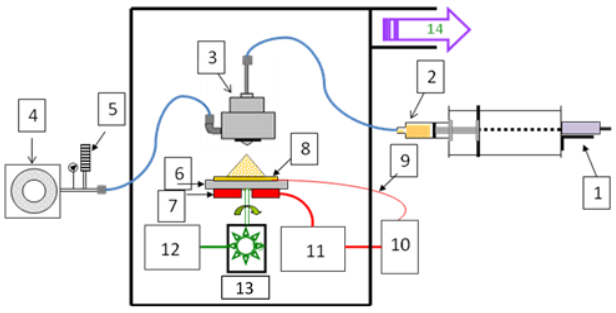

Figure (1): Sketch of the spray pyrolysis set-up: 1) DC electrical motor, 2) Syringe pump, 3) Ultrasonic atomizer. 4) Oil-less air compressor, 5) Flow meter, 6) Rotating holder, 7) Heater, 8) Substrate, 9) Thermocouple, 10) Temperature controller, 11) AC power supply, 12) DC power supply, 13) Motor and 14) Gas exhaust outlet.

The substrates were cleaned subsequently with toluene, ethanol, hot diluted HCl and distilled water then finally ultrasonic cleaning was applied. [22] The sprayed solution is prepared by dissolving the stoichiometric ratios of the precursor into solvent using a magnetic stirrer. The prepared solution was then pumped through a home-made syringe pump to a 48 kHz ultrasonic atomizer, SONO.TEK, toward a heated substrate that is rotated during deposition for film homogeneity. The components of the used home-made set up are schematically depicted in Figure (1).

2.3. Optimization of Preparation Parameters

There are many parameters that affect the film formation, thus, two categories of the preparation parameters were considered:

i- Fixed parameters that are kept the same for all of the samples: airflow rate (15 ml/min), solution flow rate (1 ml/min), samples holder rotation (15 rpm) and substrate to nozzle distance (14 cm).

ii- Optimized parameters: different arrangements of successive steps can be proposed for optimization of the process parameters to prepare thin films by spray pyrolysis technique. Some authors attain the optimum deposition parameters by trial and error. [23] In this work, a systematic optimization of each preparative parameter has been obtained through an independent study of their influence on the obtained films. Five series of films were prepared according to the steps that are illustrated in the flow chart given in Figure (2). The starting parameters were specified depending on the average values in the literature as well as on some preliminary tests.

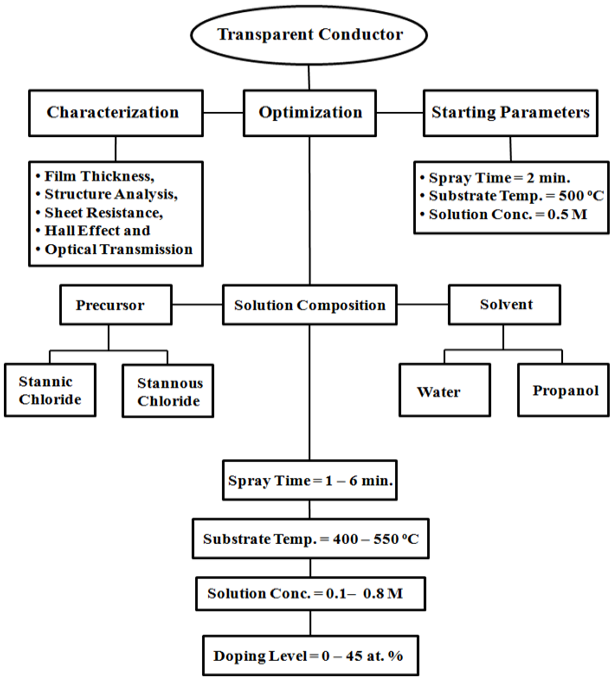

Figure (2): Flow chart of the optimization steps.

2.3.1. Solution Composition

The choice of the precursor salt and the solvent is the first important task. before the optimization of the other parameters. Two inorganic tin compounds; stannic chloride ($SnCl_4.5H_2O$) and stannous chloride ($SnCl_2$), were used as precursors with two types of solvents; water and isopropyl alcohol (2-propanol). For this purpose, two groups of solutions were examined:

- Group (I); dissolving stannic chloride into the two different solvents.
- Group (II); dissolving stannous chloride with the same molarity as stannic in the two solvents.

For the two groups, the other parameters are kept constant at: spray time = 2 min., substrate temperature = 500 ^oC and solution concentration = 0.5 M.

2.3.2. Spray Time

A series of tin oxide films was prepared using different deposition times from 1 to 6 min in steps of 1 minute. Other preparation parameters were fixed at: the optimum solution composition obtained from the first step, substrate temperature = 500 ^oC and solution concentration = 0.5 M.

2.2.3. Substrate Temperature

A series of SnO_2 films was deposited at different substrate temperatures in the range from 400 to 550 ^oC in steps of 25 ^oC. The other preparation parameters were fixed at the optimum solution composition and spray time obtained from the first and second steps, respectively, and solution concentration = 0.5 M.

2.3.4. Solution Concentration

The concentration of sprayed solution was varied from 0.1 to 0.8 M. The other preparation parameters were fixed at their optimum values obtained from the previous steps.

2.3.5. Doping Level

Using the above optimum preparation parameters, the effect of doping level (at. %) by fluorine was monitored from 0 to 45 at.%.

2.4. Measurements and Characterization

The accurate measurement of film thickness was achieved by multiple–beam Fizeau fringes at reflection method using a monochromatic beam, λ= 546 nm, from an Hg-Lamp. For the structural characterization, X-ray diffraction patterns of the prepared films onto glass substrate were collected at room temperature by $\theta/2\theta$ Diano diffractometer with Fe-filtered Co-K_α radiation (λ = 0.179 nm) at 50 kV and 20mA. Step scanning with step size of 0.1^o (2θ) and counting time of 3 second per step was used for the entire 2θ-range. Size and strain information were determined by the profile analysis of the X-ray peaks using Winfit program. [24] The values of the pole density P_{hkl} of the different (hkl) planes were estimated from the observed diffraction integrated intensities using the following equation: [25, 26]

$$P_{hkl} = \frac{I_{hkl}}{I_{r,hkl}} / \frac{1}{n} \sum \frac{I_{hkl}}{I_{r,hkl}}$$

where I_{hkl} and $I_{r,hkl}$ is the integrated intensity in the observed powder diffraction and random sample, respectively, and n is the number of reflections. The accurate integrated intensity and peak positions, 2θ, were extracted from the experimental diffractograms using WinFit program.

The optical transmittance, T (λ), was measured using double-beam Jasco V-530 UV/Vis spectrophotometer in the wavelength range of 400 – 800 nm. Van der Pauw technique was used for sheet resistance measurement. For Hall Effect investigation, a magnetic field *B* of 0.58 Tesla was induced and a bias current of 7 mA was applied. A square sample (0.5 x 0.5 mm^2) was used and the bias current was applied from a highly stable power supply (Keithley 238 high current source/voltage measure unit) while the potential and Hall voltage was measured by a Keithley 617 programmable electrometer.

3. Result and Discussion

3.1. Un-doped SnO_2

3.1.1. Precursor and Solvent

The first step in the optimization was to explore the effect of chemistry of the sprayed solution in order to select the appropriate precursor materials and solvent to produce the best performing undoped SnO_2 films as a transparent conducting electrode. Two precursors with two different solvents were used to prepare the sprayed solution. All the preparation parameters were kept constant at the starting parameters given above.

A) Structural Characterization

X-ray diffractograms of the prepared films are shown in Figure (3). In all cases, the films are polycrystalline of single tetragonal SnO_2 phase. According to the values of the pole densities, the (301) plane (P_{301} = 2.5 - 2.9) is the most preferentially oriented one parallel to the film surface. The variation of precursor (stannic/stannous) did not change the preferred orientation in contrast with Amma *et al*., who observed an effect for the starting compound. [22] However, the variation of solvent, water/propanol, changes the type of preferred orientation to (200) (P_{200} = 1.2 - 2.2) and (211) (P_{211} = 1.2 – 1.4) in case of water and propanol, respectively, i.e. it depends mainly on the solvent. On the other hand, the crystallite size, given in Table (1), is smaller in case of water than propanol as a solvent and in case of stannic than of stannous as a precursor. Thus, the crystallographic orientation depends on the solution chemistry

(precursor/solvent) [27] and also the crystallite size is affected.

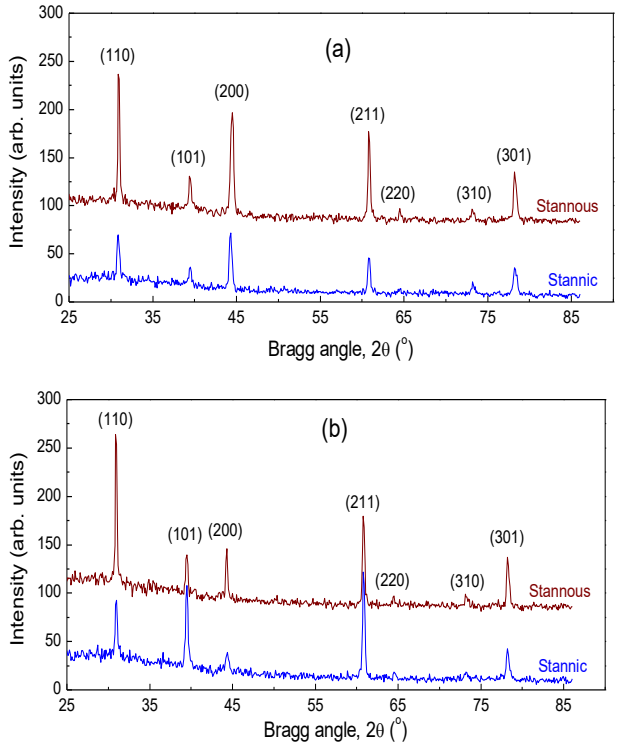

Figure (3): X-ray diffractograms for SnO_2 films prepared using different precursors (stannous and stanic) and solvents: (a) Water and (b) Propanol.

Table 1: Crystallite size (nm) of SnO_2 films prepared from different precursors and solvents.

Solvent	Precursor	
	Stannic	Stannous
Water	20.7	22.7
Propanol	24.1	29.3

B) Electrical and Optical Properties:

The electrical characteristics, sheet resistance, R_s, and carrier density, n, of the four different cases are given in Table (2). Comparing the two solvents, the sheet resistance was observed to be lower in the case of water, due to the higher carrier concentration and may be also due to the formation of (200) oriented growth. [3] The lower resistance in case of stannic than stannous, when water was used, is as well due to the high carrier concentration. However, in case of propanol, it seems that the effect of the decrease in mobility due to the smaller crystallite size in case of stannic overcomes that of the increase in the carrier concentration. Resistivity of films, R_s, is mainly inversely proportional to both the carrier density, n, and mobility, μ. Many scattering mechanisms affect the mobility as those attributed to the scattering of grain boundaries, charged impurities or lattice defects in addition to that of lattice as usually expected in the extrinsic doped semiconductors. On the other hand, the relation between μ and n is not linearly proportional; one parameter may increase while the other decreases. Thus, their product is the main effect on resistance.

The optical transmission in the UV/VIS range was generally higher in case of propanol as a solvent (64 – 90%) than that of water and in case of stannic as a precursor than stannous (48 – 85%). The transmission values at λ = 550 nm, T_{550}, of the four cases are given in Table (2). It is clear that it is higher in case of propanol than water as a solvent and for of stannic than stannous as a precursor.

Table (2): Sheet resistance (R_s), carrier density (n), transmission at λ = 550 nm (T_{550}) and figure of merit (ϕ_{TC}) in case of different precursors and solvents.

Solvent	R_s (Ω/□)		n ($x10^{20}$ cm^{-3})		T_{550} (%)		ϕ_{TC} ($x10^{-4}$ Ω^{-1})	
	Stannic	Stannous	Stannic	Stannous	Stannic	Stannous	Stannic	Stannous
Water	124.12	200.69	1.87	0.87	76	73	5.16	2.23
Propanol	385.49	295.78	1.37	0.43	88	83	7.32	5.50

C) Performance:

Inspection of Table (2) shows that the increase of the transmission (T_{550}) is more effective than the decrease of the sheet resistance in improving the performance (high value of figure of merit ϕ_{TC}) of the transparent conductive electrodes. In the following steps of optimization, the stannic as the precursor and propanol as the solvent will be used.

3.1.2. Effect of Spray time

The spray time was varied from 1- 6 min, using propanol as a solvent while the concentration of the precursor and the substrate temperature were kept constant at 0.5 M and 500 °C, respectively.

A) Film Thickness and Structure Characteristics:

A continuous linear increase in film thickness was observed with increasing the deposition time. This is normal, where larger amount of materials were deposited with longer time. X-ray diffraction patterns of the prepared films at different deposition times are shown in Figure (4). The diffractograms proved that all films possess polycrystalline single phase of a tetragonal structure. The overall diffraction peak intensities are enhanced as the spray time increases, which is attributed to the observed increase in the film thickness. The spray time affected only the degree of preferred orientation but did not affect the observed type that is (211) (P_{211} = 1.26 – 1.66) and (301) (P_{301} = 1.84 – 3.26). Thus, the spray time affects the overall diffraction intensity and the degree of preferred orientation but not the type.

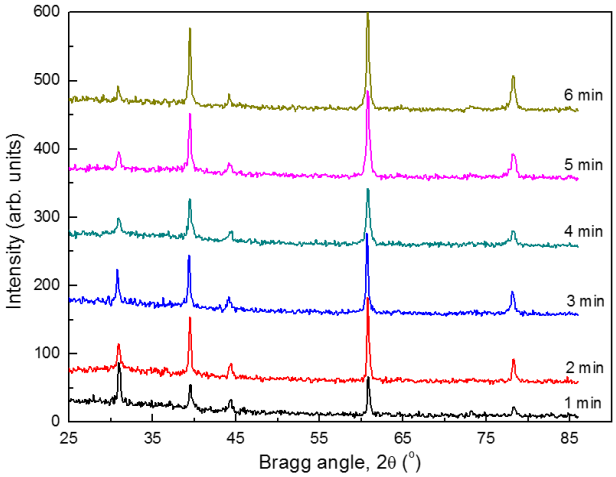

Figure (4): X-ray diffractograms of SnO_2 films prepared at different spray times.

B) Electrical and Optical Properties:

A small increase of carrier density was observed from 9.0 x 10^{19} to 13.9 x 10^{19} cm^{-3} with increasing the spray time while the sheet resistance, R_s, was decreased rapidly during the first two minutes and then slightly decreased as depicted in Figure (5). This is the thickness-dependent of resistivity of the thin films. Thus, as the film thickness increases, electrical resistance becomes thickness independent. Therefore, the decrease in the sheet resistance with increasing the deposition time is mainly attributed to the increase of thickness with time and slightly to the increase of the carrier density.

Figure (6) shows the transmission spectra in the visible region for films deposited with different spray times. A remarkable descending of the transmission is observed as the spray time increases. This decrease in optical transmission is mainly due to the increase of the film thickness.

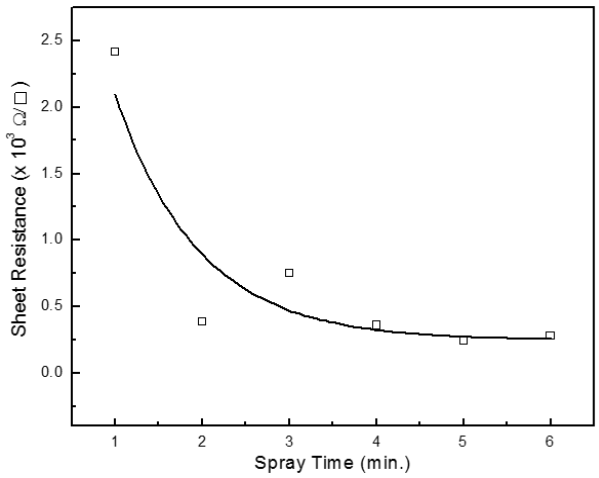

Figure (5): Effect of spray time on sheet resistance (the line is guide to the eye).

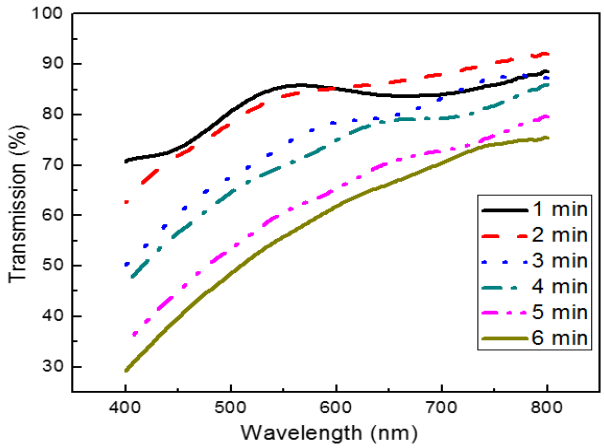

Figure (6): The influence of the spray time on transmission.

C) Performance:

Using the electrical and optical results, the figure of merit was calculated and depicted in Figure (7). Although the transmission decreases with increasing the spray time (Figure (6)), the sheet resistance decreases (Figure (5)). The compromise gives the optimum value at 2 min., that is the time at which the sheet resistance is minimum and becomes thickness independent while T_{550} still decreases. This spray time will be considered in the subsequent steps.

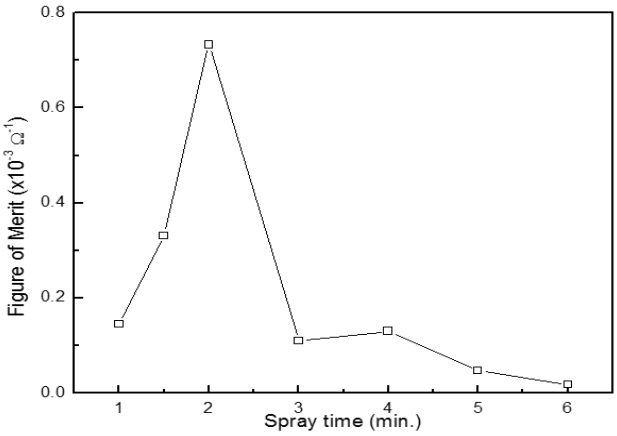

Figure (7): The figure of merit at different spray times

3.1.3. Effect of Substrate Temperature

Substrate temperature was varied from 400 – 550 ºC, while the other conditions and parameters were kept constant at those optimized before; propanol as a solvent and a spray time of 2 min. At the same time, the concentration of the solution was kept constant at 0.5 M.

A) Film Thickness and Structure Characteristics

Figure (8) illustrates the variation of film thickness as a function of the substrate temperature. Almost there is no change in film thickness up to substrate temperatures ≤ 450 ºC. However, at higher temperatures > 450 ºC, a considerable increase in thickness was realized. This

indicates that the growth rate of SnO_2 is enhanced as the substrate temperature ascends and that the reaction to form SnO_2 is accomplished over 450 °C.

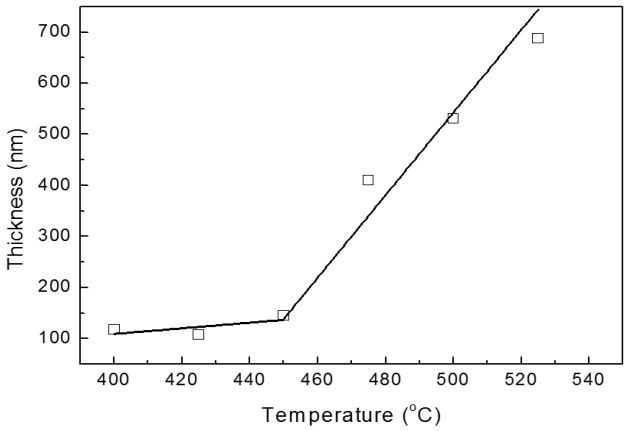

Figure (8): The change of film thickness with substrate temperature (the line is guide to the eye).

The diffractograms of the prepared films at different substrate temperatures are shown in Figure (9) and the variation of the integrated intensity and the breadth are illustrated in Figure (10). All samples adopted polycrystalline single phase of a tetragonal structure and the formation of SnO_2 was accomplished at temperatures ≥ 450 °C. On the other hand, the crystallinity improved and the crystallite size increases (10 – 25 nm) with temperature as indicated by the increase in peak intensity and a decrease in the breadth. Films prepared at temperature ≥ 475 °C were well crystalline and the overall intensities were enhanced as the temperature increases due to the increase of film thickness. It was also found that the temperature did not affect the type but only the degree of preferred orientation (P_{211} = 1.08 – 1.71 and P_{301} = 1.40 – 2.99).

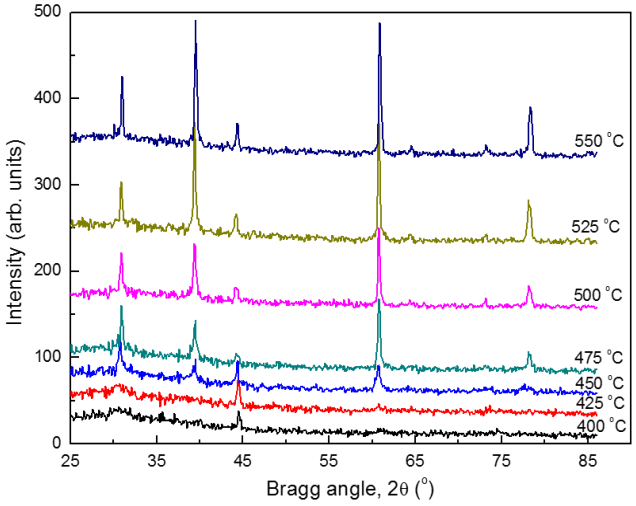

Figure (9): X-ray diffractograms for SnO_2 films prepared at different substrate temperatures.

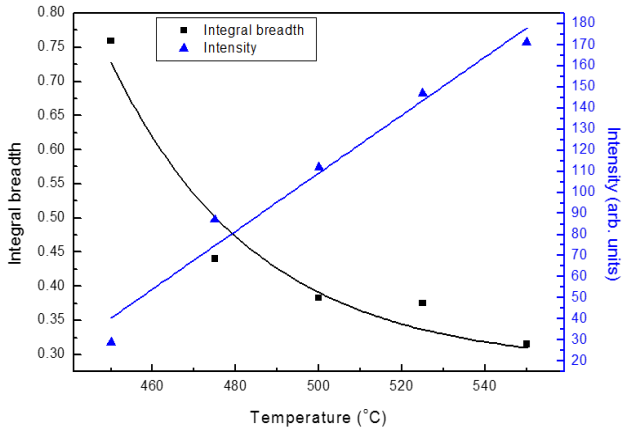

Figure (10): Variation of intensity and breadth of (211) diffraction peak with the variation of substrate temperature (the line is guide to the eye).

B) Electrical and Optical Properties

It was found that the carrier density decreased from 37.1 x 10^{19} to 8.7 x 10^{19} cm^{-3} as the temperature ascended, although the sheet resistance decreased rapidly up to 450 °C as depicted in Figure (11). The decrease of the carrier density can be attributed to the vacancy annihilation. Using Kroger-Vink notation, this is formulated as:

$$V_O^{\bullet\bullet} \rightarrow O_O^x - 2e^-$$

One has to expect that this decrease bring about an increase of the sheet resistance. However, the effect of increasing of the film thickness as well as the increase in the crystallite size with temperature, which in turn enhances the film mobility [28], results in a decrease in the sheet resistance. So, the integration of characteristics from the different measurements (thickness, structure and Hall Effect) leads to the conclusion that the effect of thickness and mobility on sheet resistance is predominant within the substrate temperature range of 400-450 °C. Using substrate temperature higher than 450 °C, the sheet resistance becomes thickness-independent and the effect of the carrier density going to be the predominant one that causing the observed slight increase of the sheet resistance.

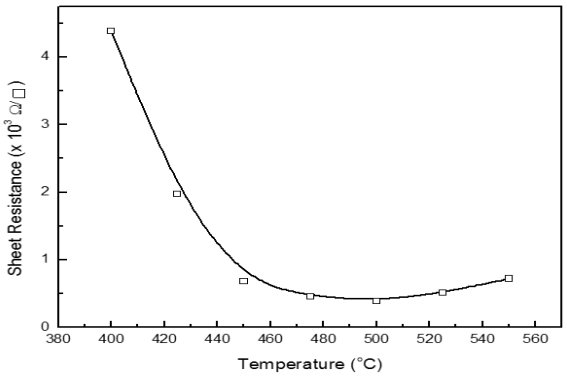

Figure (11): Effect of substrate temperature on sheet resistance.

Figure (12) shows the transmission spectra in the visible region for films prepared at different substrate temperatures. The transmission, T_{550}, is almost in the range of 70- 85 %. No pronounced dependence on substrate temperature was observed at lower substrate temperatures with a slight decrease at a high temperature of 550 °C. This seems to be due to the increase of film thickness.

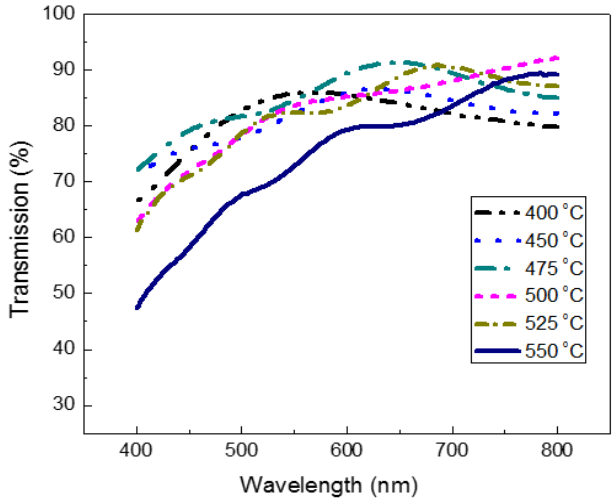

Figure (12): The influence of the substrate temperature on transmission.

B) Performance

Relying again on the electrical and optical results, the figure of merit was calculated and depicted in Figure (13). The optimum values were found in the temperature range of 475 – 500 °C, that is the range of minimum sheet resistance. The subsequent decrease in Φ_{TC} is due to the decrease in T_{550}. A substrate temperature of 500 °C has been used in the next step as the optimum one.

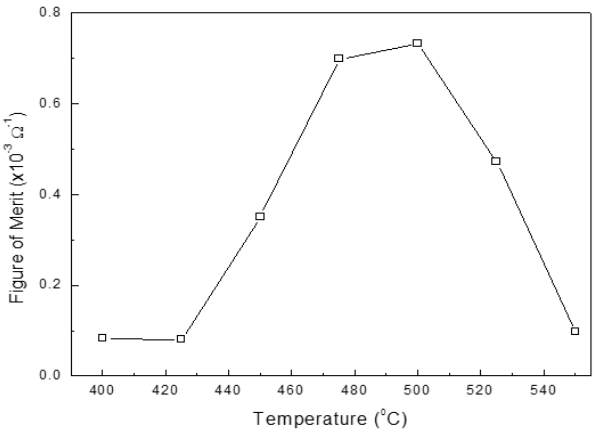

Figure (13): Figure of merit of SnO_2 prepared at different substrate temperatures.

3.1.4. Effect of Solution Concentration

In order to study the effect the of the sprayed solution concentration, molarity was varied from 0.1 to 0.8 M, while the other conditions and parameters that are optimized before were kept constant using propanol as a solvent, spray time of 2 min. and a substrate temperature of 500 °C.

A) Film Thickness and Structure Characteristics

As the concentration of $SnCl_4$ in spraying solution increases in the given range, a continuous linear increase in the film thickness from 130 to 800 nm was observed. This is mainly attributed to the relative increase of Sn^{4+} in the solution that enhances the growth rate. [5, 29] The diffractograms of the prepared samples with different solution concentrations were shown in Figure (14). All samples are of a polycrystalline single phase of a tetragonal structure. The prepared films are crystalline but the overall intensities are enhanced with the increase of the spraying solution concentration. This is because the amount of deposited SnO_2 is greater as the concentration increases; as being reflected in the increase of the film thickness.

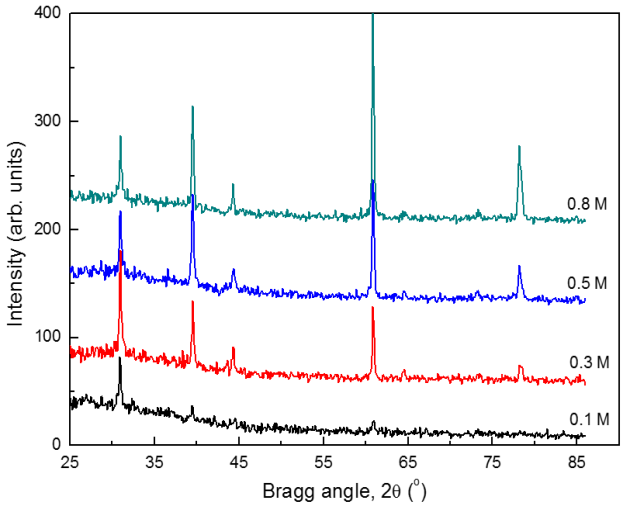

Figure (14): X-ray diffractograms of SnO_2 films prepared with different concentrations of sprayed solution.

B) Electrical and Optical Properties:

An increase in carrier density from 5.3 x 10^{19} to 14.6 x 10^{19} cm^3 was detected. The variation of sheet resistance with concentration for sprayed $SnCl_4$ solution is shown in Figure (15). The sheet resistance decreased abruptly up to 0.2 M and then turned to be a concentration independent at higher concentration. That increase of the carrier density indicates likewise the increase in oxygen vacancies. The decrease of R_s with concentration was attributed to the increase of the carrier concentration and film thickness.

Figure (16) shows the optical transmittance spectra in the visible region. The films show moderate transmittance between 65 and 90 % at wavelength of 550 nm. Generally, as the concentration of $SnCl_4$ increases the transmittance goes to decrease due to the increase of the film thickness.

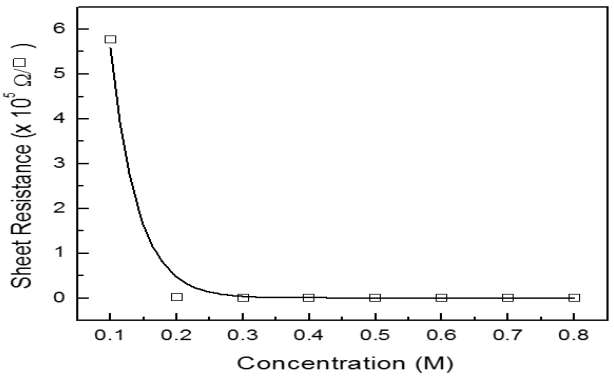

Figure (15): Effect of solution concentration on sheet resistance.

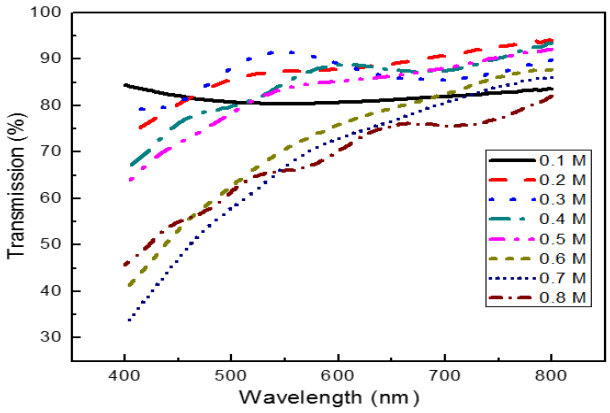

Figure (16): Influence of the concentration on the optical transmission of SnO_2 films.

C) Performance:

The figure of merit was calculated and depicted in Figure (17), based on the electrical and optical properties. The optimum concentration was found to be 0.3 M.

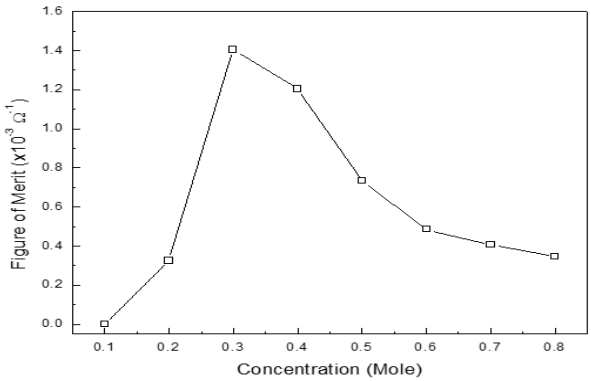

Figure (17): The figure of merit of Sno_2 films at different solution concentrations.

Low performance at concentrations < 0.3 M is mainly due to the high sheet resistance. On the other hand, the decrease in performance at concentration > 0.3 M is attributed to the decrease in optical transmission. This optimum value signifies the solution concentration in the range of the minimum sheet resistance and the maximum value of T_{550}.

3.2. Fluorine Doped SnO_2

The influence of fluorine doping level (0-45 at. %) on the structural as well as the optical and the electrical properties of SnO_2 films prepared by the above optimized conditions (solvent= 2-propanol, Spray time= 2 min., substrate temperature = 500 °C and concentration = 0.3 M) was studied and the results are established in this section.

A) Film Thickness and Structural Characteristics:

Figure (18) shows the effect of F-doping on thickness. There was an increase in the film thickness up to doping concentration = 25 at. % and as it exceeds this doping level, the film thickness decreases. This is in agreement with the observations of Moholkar *et al.* [30]

During the initial continuous increase of thickness, the film grows by adsorption followed by a reaction of Sn containing species with the adsorbed H_2O molecules:

$$SnCl_4 + 2H_2O \rightarrow SnO_2 + 4HCl \quad (3)$$

The decomposition of ammonium fluoride takes place simultaneously and forms a cloud of HF according to the following:

$$NH_4F \rightarrow NH_3 + HF \quad (4)$$

This leads to the reaction:

$$SnO_2 + 4HF \leftrightarrow SnF_4 + 2H_2O$$

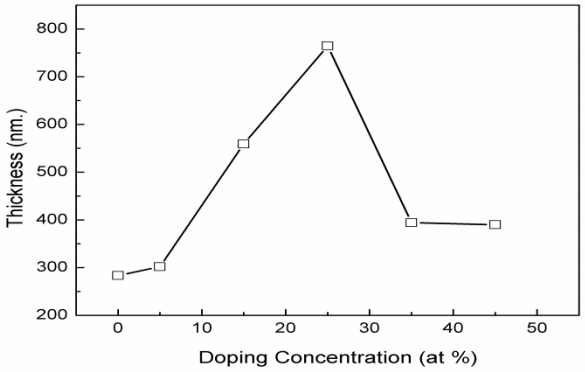

Figure (18): Effect of doping concentration on film thickness.

According to the law of mass action, the added dopant determines the rate of deposition of SnO_2 films. [31] It was suggested that when the F concentration is too high, the available oxygen from H_2O molecules is insufficient to increase the growth rate, i.e. a decrease in the film thickness is expected. [28] Therefore, the doped films prepared by different doping level results in different growth rate and consequently different film thickness depending on the ammonium fluoride concentration.

From the X-ray diffractograms shown in Figure (19), all the prepared films of fluorine-doped tin oxide (FTO) are polycrystalline single phase of a tetragonal structure. Thus, the doping level in the studied range did not change the crystal structure. However, it was found that the increase of the doping level changing the type of preferred orientation from (301) + (211) to (301) + (200). Yet, no considerable change of the calculated cell volume was observed due to the very slight difference between the ionic radius of O^{-2} = 1.36 Å^3 and F^- = 1.33 Å^3.

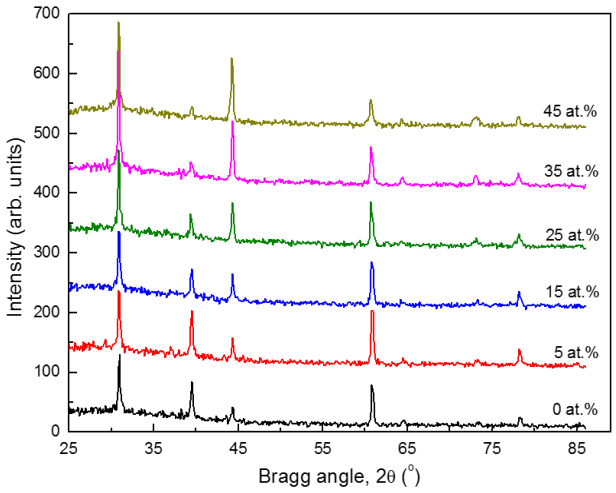

Figure (19): X-ray diffractograms of SnO_2 films prepared with different concentrations of F-doping.

A) Electrical and Optical Properties:

It was found that carrier concentration was increased from 1.1 x 10^{20} to 5.0 x 10^{20} cm^3 as the fluorine doping ratio was increased. The sheet resistance, R_s, is generally decreased but specifically up to a doping level of 25 at.% as depicted in Figure (20). In order to discuss this behaviour, three possibilities have to be considered. Using Kröger-Vink notation [32], the possible processes can be represented as:

(1) F^- anion introduced into the O-vacancies site according to the following formula:

$$V_O^{\bullet\bullet} \rightarrow F_O^{\bullet} - e^{/}$$

This leads to a decrease of the free electrons, i.e. an increase in the resistivity.

(2) F^- anion occupying interstitial sites according to the following formula:

$$V_I^{\times} \rightarrow F_I^{/} - e^{/}$$

This is acting as acceptors leading also to a decrease in the free electrons as occurs with the possibility (1) and consequently an increase in the resistivity.

3) F^- anion substitute O^{-2} anion according to the following formula:

$$O_O^{\times} \rightarrow F_O^{\bullet} + e^{/}$$

This is acting as donors in the lattice and introduces more free electrons, i.e. a decrease in the resistivity.

Therefore, processes (1) and (2) are unlikely to occur while process (3) is reasonable and most likely to occur. Thus, fluorine ions occupy the oxygen sites in the SnO_2 lattice creating free electrons giving an increase in the charge carriers and a decrease of electrical resistivity. However, the slight increase in resistivity at doping level higher than 25t%, a slight increase in resistivity is observed (inset of Fig.(20) due to the decrease in film thickness (Fig. 18), that overcome the effect of the increase of carrier concentration

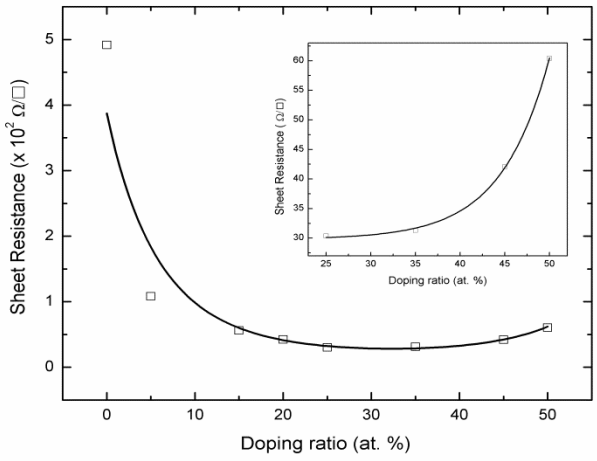

Figure (20): Effect of doping concentration on sheet resistance.

Figure (21) shows the optical transmittance spectra in the visible region for FTO films of different doping level. Generally, all samples have a high transmission between 80 to 90 %. However, a very slight decrease in the transmission (T_{550}) was observed as the doping level ascends.

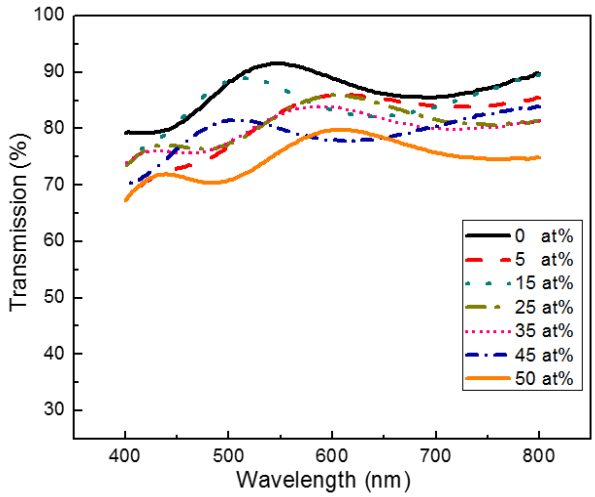

Figure (21): The influence of the doping concentration on transmission.

C) Performance

The figure of merit of FTO films is presented in Figure (22). For doping level up to 25 at. %, the main effect was the decrease of the sheet resistance (≈ 90 %) rather than the change of transmission (≈11 %). Although the transmission decrease, the abrupt decrease in sheet resistance results in improving the performance. At doping levels above 25 at. %, the slight increase in the sheet resistance, as depicted in Figure (20), in addition to the decrease in transmission deteriorates the performance. So that, the optimum value from the curve is that at 27 at. %.

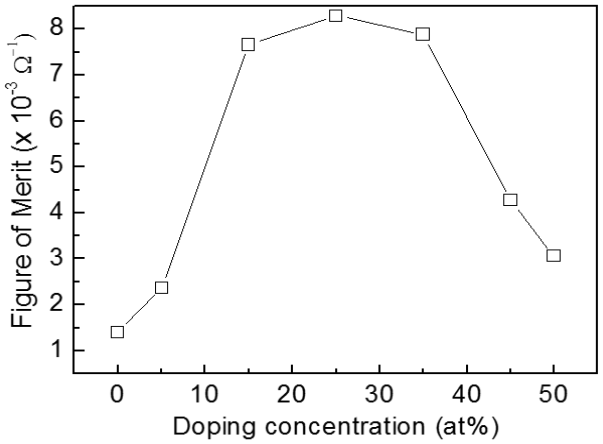

Figure (22): Effect of doping concentration on the performance (figure of merit) of the FTO as transparent electrode.

4 Conclusions

Correlation, combination and integration of the results from different measurements leads to the following conclusions. The polycrystalline single phase of a tetragonal structure is formed under all the used preparation conditions with enhancement of crystallinity as the substrate temperature exceeds 450 ºC. Thickness of the films is continuously increasing with increasing the spray time, the substrate temperature and the sprayed solution concentration. However, it shows a maximum at fluorine doping level of 25 at. %. Both the type of solvent (solution chemistry) and doping level affect the type of the crystallographic texture (preferred orientation). Sheet resistance and carrier density are affected by both the precursor and solvent. Sheet resistance decreases by the spray time, the substrate temperature, the solution concentration and the doping level. On the other hand, the carrier concentration slightly increases with the spray time, the solution concentration and the doping level but decreases with the substrate temperature. The optical transmission is higher in case of stannic and 2-propanol and it decreases with the increase of all the preparation parameters and doping level but there is no considerable affect noticed for the substrate temperature. The increase of the transmission (T_{550}) is more effective than the decrease of sheet resistance in improving the performance of the transparent conductive electrodes. The optimum conditions for the maximum performance of F:SnO_2 as transparent conducting electrode are specified as: 1) Precursor: stannic chloride, 2) Solvent: propanol, 3) Spary time: 2 min, 4) Substrate temperature: 500 ºC, 5) Solution concentration: 0.3 M and 6) Doping concentration: 27 at. %.

References

[1] A.I. Martine z, D. R. Acosta, Effect of the fluorine content on the structural and electrical properties of SnO_2 and ZnO−SnO_2 thin films prepared by spray pyrolysis, Thin Solid Films 483 (2005) 107-113.

[2] A. A. Yadav, E. U. Masumdar, A. V. Moholkar, M. Neumann-Spallart, K. Y. Rajpure, C. H. Bhosale, Electrical, structural and optical properties of SnO2:F thin films: Effect of the substrate temperature, Journal of Alloys and Compounds 488 (2009) 350-355.

[3] A. Agashe, S.Mahamuni, Competitive effects of film thickness and growth rate in spray pyrolytically deposited fluorine-doped tin dioxide films, Thin Solid Films 518 (2010) 4868-4873.

[4] A. A. Yadav, E. U. Masumdar, A. V. Moholkar, K. Y. Rajpure, C. H. Bhosale, Effect of quantity of spraying solution on the properties of spray deposited fluorine doped tin oxide thin films, Physica B 404 (2009) 1874-1877.

[5] A. V. Moholkar, S. M.Pawar, K. Y. Rajpure, C. H. Bhosale, Effect of concentration of $SnCl_4$ on sprayed fluorine doped tin oxide thin films, Journal of Alloys and Compounds 455 (2008) 440-446.

[6] M. A. Aouaj, R. Diaz, A.Belayachi, F. Rueda, M. Abd-Lefdil, Comparative study of ITO and FTO thin films grown by spray pyrolysis, Materials Research Bulletin 44 (2009) 1458-1461.

[7] J. Xu, S. Huang, Z.Wanga, First principle study on the electronic structure of fluorine-doped SnO2, Solid State Communications 149 (2009) 527-531.

[8] P. Veluchamy, M. Tsuji, T. Nishio, T.; Aramoto, H. Higuchi, S. Kumazawa, S. Shibutani, J. Nakajima, T. Arita, H.Ohyama, A.Hanafusa, T, Hibino, K.Omura, A pyrosol process to deposit large-area SnO_2:F thin films and its use as a transparent conducting substrate for CdTe solar cells, Solar Energy Materials & Solar Cells 67 (2001) 179-185.

[9] E. Comini, G. Fagila, G. Sberveglier, UV light activation of tin oxide thin films for NO_2 sensing at low temperatures, Sensors and Actuators B: Chemical 78 (2001) 73-77.

[10] J. H. Lee, N.-G. Park and Y.-J. Shin, Nano-grain SnO_2 electrodes for high conversion efficiency SnO_2−DSSC, Solar Energy Materials and Solar Cells 95 (2011) 179-183.

[11] S. J. Ikhmayies and R. N. Ahmad-Bitar, The effects of post-treatments on the photovoltaic properties of spray-deposited SnO_2:F thin films, Applied Surface Science 255 (2008) 2627-2631.

[12] S. I. Boiadjiev, G. H. Dobrikov and M. M. Rassovska, Preparation and properties of RF sputtered indium−tin oxide thin films for applications as heat mirrors in photothermal

solar energy conversion, Thin Solid Films 515 (2007) 8465-8468.

[13] E. Zelazowska and E. Rysiakiewicz-Pasek, Thin TiO_2 films for an electrochromic system, Optical Materials 31 (2009) 1802-1804.

[14] V. Bilgin, I. Akyuz, E. Ketenci, S. Kose and F. Atay, Electrical, structural and surface properties of fluorine doped tin oxide films, Applied Surface Science 256 (2010) 6586-6591.

[15] Agashe, J. Hupkes, G. Schope and M. Berginski, Physical properties of highly oriented spray-deposited fluorine-doped tin dioxide films as transparent conductor, Solar Energy Materials & Solar Cells 93 (2009) 1256-1262.

[16] T. Fukano and T. Motohiro, Low-temperature growth of highly crystallized transparent conductive fluorine-doped tin oxide films by intermittent spray pyrolysis deposition, Solar Energy Materials & Solar Cells 82 (2004) 567-575.

[17] E. Elangovan and K. Ramamurthi, Studies on optical properties of polycrystalline SnO_2:Sb thin films prepared using $SnCl_2$ precursor, Cryst. Res. Technol. 38 (2003) 779-784.

[18] A. Kurz, K. Brakecha, J. Puetz and M. A. Aegerter, Strategies for novel transparent conducting sol−gel oxide coatings, Thin Solid Films 502 (2006) 212-218.

[19] P. Y. Liu, J. F. Chen and W. D. Sun, Characterizations of SnO_2 and SnO_2:Sb thin films prepared by PECVD, Vacuum 76 (2004) 7-11.

[20] J. Ma, X. Hao, S. Huang, J. Huang, Y. Yang and H. Ma, Comparison of the electrical and optical properties for SnO_2:Sb films deposited on polyimide and glass substrates, Applied Surface Science 214 (2003) 208-213.

[21] G. Haacke, New figure of merit for transparent conductors, J. App. Phys.47 (1976) 4086-4089.

[22] A. Jadsadapattarakul, C.Euvananont, C.Thanachayanont, J.Nukeaw, T.Sooknoi, Tin oxide thin films deposited by ultrasonic spray pyrolysis, Ceramics International 34 (2008) 1051-1054.

[23] S. D. Amma, V. K.Vaidyan, P, K,Manoj, Structural, electrical and optical studies on chemically deposited tin oxide films from inorganic precursors, Materials Chemistry and Physics 93 (2005) 194-201.

[24] S. Krumm: (a) An Interactive Windows Program for Profile Fitting and Size/Strain Analysis, Materials Science Forum 183 (1996) 228-231, and (b) The Erlangen geological and mineralogical software collection, Computers and Geosciences 25 (1999) 489-499.

[25] G. B. Harris, X. Quantitative measurement of preferred orientation in rolled uranium bars, Pil. Mag. 43 (1952) 113-123.

[26] C. S. Barrett, T. B. Massaliski, Structure of Metals, third revised edition, Pergamon Press, Oxford, (1980) ch. 9, p. 204-205.

[27] A. Smith, J. M. Laurent, D. S. Smith, J. P. Bonnet, R. R. Clemente, Relation between solution chemistry and morphology of SnO_2-based thin films deposited by a pyrosol process, Thin Solid Films 266 (1995) 20-30.

[28] A. V. Moholkar, S. M.Pawar, K. Y.Rajpure, P. S.Patil, C. H.Bhosale, Properties of highly oriented spray-deposited fluorine-doped tin oxide thin films on glass substrates of different thickness, Journal of Physics and Chemistry of Solids 68 (2007) 1981-1988.

[29] A. Agashe, M. G.Takwale, V. G.Bhide, Effect of Sn incorporation on the growth mechanism of sprayed SnO2films, Journal of Applied Physics 70 (1991) 7382-7386.

[30] A. V. Moholkar, S. M.Pawar, K. Y.Rajpure, C. H.Bhosale, J. H. Kim, Effect of fluorine doping on highly transparent conductive spray deposited nanocrystalline tin oxide thin films, Applied Surface Science 255 (2009) 9358-9364.

[31] A. Agashe, S. S. Major, Effect of heavy doping in SnO_2:F films, Journal of Material Science 31 (1996) 2965-2969.

[32] F. A. Kroger, H. J.Vink, Relations between the Concentrations of Imperfections in Crystalline Solids, Solid State Physics 3 (1956) 307-435.